# CHEMISTRY
## A European Journal

www.chemeurj.org


Reprint

A Journal of
ChemPubSoc Europe
ACES
Asian Chemical Editorial Society
WILEY-VCH

ChemPubSoc Europe

DOI: 10.1002/chem.201903704

CHEMISTRY A European Journal Communication

Click Chemistry

# Synthesis and Cellular Labeling of Caged Phosphatidylinositol Derivatives

Rainer Müller[+],[a] Mevlut Citir[+],[a] Sebastian Hauke,[a] and Carsten Schultz*[a, b]

**Abstract:** Phosphatidylinositol (PI) is the biosynthetic precursor for seven phosphoinositides, important signaling lipids in cells. A membrane-permeant caged PI derivative featuring a photo-removable coumarinyl group masking the negative charge of the phosphate, as well as two enzymatically removable butyrate esters for increased lipophilicity and for preventing phosphate migration, were synthesized. Rapid cell entry and cellular labeling in fixed cells was demonstrated by a photo-cross-linkable diazirine followed by attachment of a fluorophore through click chemistry. Using this technique, we found that the multifunctional caged PI derivative resided predominantly at internal membranes but rapidly changed to the plasma membrane after uncaging. Accordingly, a preliminary proteomic analysis of the lipid–protein conjugates revealed that the two major PI transport proteins PITPα and β were prime targets of the photo-cross-linked PI derivative.

Photo-activatable ("caged") lipid derivatives are important tools in cell biology through which the concentration of a specific lipid species can be elevated by a flash of light, if appropriate with subcellular resolution.[1] The typical photo-removable groups used for lipids were nitroveratryl and 7-diethylamino-4-methylene-coumarin groups.[2] The latter is often preferred, because the coumarin is a fluorophore, which is handy for monitoring and quantifying cell entry of the caged compound.

[a] *Dr. R. Müller,[+] Dr. M. Citir,[+] Dr. S. Hauke, Prof. Dr. C. Schultz*
*Cell Biology & Biophysics Unit*
*European Molecular Biology Laboratory (EMBL)*
*Meyerhofstrasse 1, 69117 Heidelberg (Germany)*
*E-mail: schultz@embl.de*

[b] *Prof. Dr. C. Schultz*
*Department of Chemical Physiology and Biochemistry*
*Oregon Health & Science University*
*3181 SW Sam Jackson Park Rd, Portland, OR 97239-3098 (USA)*
*E-mail: schulcar@ohsu.edu*

[+] *These authors contributed equally to this work.*

*Supporting information and the ORCID identification number(s) for the author(s) of this article can be found under: https://doi.org/10.1002/chem.201903704.*



Phosphoinositides (PIPx) are quite rare lipids that serve as membrane-bound anchors for a variety of proteins carrying specific lipid-recognizing domains, such as PH domains for $PIP_2$ and $PIP_3$ isoforms, PX domains for PI(4)P and FYVE domains for PI(3)P.[3] Their biosynthesis is spread out over various cellular membrane systems and in all cases starts from phosphatidylinositol (PI). Most phosphoinositides are well studied but the functions of PI beyond serving as the biosynthetic precursor for other phosphoinositides are elusive. To date, no binding domain able to specifically recognize PI has been described. However, a class I PI transport protein (PITP) is responsible for transferring PI from the ER to the plasma membrane and therefore might be considered a PI-binding protein.[4] For this reason, we aimed at preparing a set of tools, namely, photo-cross-linkable PI derivatives that are able to capture proteins binding to the lipid. In the past, we successfully used diazirine groups attached to the alkyl fatty acid tails. In addition, we always attached a terminal alkyne group useful for fluorescent labeling of the lipid in fixed cells.[5–7] Although lipids are usually washed out during the fixation process, photo-cross-linked lipids covalently attach to their binding proteins and stay at the location at the time of cross-linking. Fluorescent labeling via the alkyne allows for imaging the lipid location with high spatial precision. This technique is also useful for correlative light and electron microscopy.[7]

To provide membrane permeability, the negative charge of the phosphate bridging the inositol ring to the diacylglycerol needed to be masked with a removable group.[8] We decided to use typical bioactivatable acetoxymethyl (AM)[9] and acetoxybenzyl (AB) esters,[10] as well as a photo-removable coumarin that would permit the rapid elevation of PI levels with a flash of light through the objective of a fluorescence microscope inside intact cells.[11] All membrane-permeant phosphoinositides synthesized in the past relied on butyrates for masking the hydroxyl groups of the inositol ring.[12–14] Inside cells, butyrates are cleaved by endogenous hydrolases much slower than acetoxymethyl esters.[15] As a result, phosphate migration, which was observed for phosphate triesters, is avoided.[16] In the case of PI, masking all five hydroxyl groups would likely introduce a high amount of unnecessary lipophilicity, as well as the requirement for five enzymatic hydrolysis steps. Therefore, we aimed for introducing only two butyrates at the hydroxyl groups 2 and 6, vicinal to the single phosphate ester. This required a hydroxyl protecting group that is safely removed in the presence of phosphate triesters. For the first time, we used a fluorenylmethyl oxycarbonyl (Fmoc) group as protecting group for secondary alcohols of inositol.

 

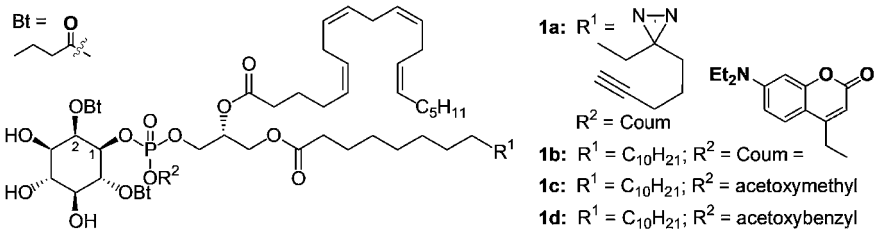


**Figure 1.** Functionalized membrane-permeant PI derivatives including the trifunctional caged derivative **1a** for photo-cross-linking and tagging by click chemistry, as well as caged (**1b**) and membrane-permeant bioactivatable derivatives (**1c**, **d**).

The resulting functionalized lipid derivatives (Figure 1) hold great promise as tools to manipulate lipid levels, to visualize lipid location in intact cells, and to fish for lipid-binding proteins via biotin conjugation and avidin beads or direct conjugation to azide beads and subsequent proteomic analysis.[6,17–19]

In previous synthetic designs of caged phosphoinositides bearing several phosphates, we used a single coumarin protecting group attached to one of the phosphates to block biological activity and masked the remaining negative charges by AM esters to provide membrane permeability.[13,14] In the case of PI, it seemed appropriate to use the caging coumarin group for masking the single negative charge of the phosphoric acid diester. As was discussed above, we aimed for esterifying the vicinal hydroxyl groups on the inositol ring in positions 2 and 6 by enzymatically cleavable butyrates.

Our synthesis of the inositol headgroup (Scheme 1) started from the previously described inositol derivative **2** that was originally used in the synthesis of membrane-permeant PI(3)P derivatives.[14] To mildly remove protecting groups from the secondary inositol alcohol groups, we decided for using Fmoc groups as they can be hydrolyzed under mild basic conditions in the absence of nucleophilic amines. We introduced the first Fmoc group to the single hydroxyl group in **2** to give the fully protected compound **3**. Subsequent removal of the more labile ketal formed diol **4**, which was further reacted to the triple Fmoc-protected precursor **5**. We then removed the remaining ketal. The resulting diol **6** was treated with a butyrate orthoester to selectively give the axial 2-*O*-butyrate **7** in an overall yield of 32% from **2**. This protected headgroup was further reacted with functionalized diacylglycerol phosphoramidites (Scheme 2).

The synthesis of the diacylglycerols (DAGs), namely, the diazirine- and alkyne-bearing DAG **8** and the *sn1*-stearoyl-*sn2*-arachidonoyl glycerol (**9**) followed previously published procedures.[2,14,17] We used standard $P^{III}$ chemistry to prepare phosphoramidite intermediates useful for coupling to the protected inositol headgroup **7**. Reaction of *N*,*N*-bis(di*iso*propylamino)-chlorophosphine (**10**) with 7-diethylamino-4-hydroxymethylcoumarin (**11**) gave the phosphorbisamidite **12** carrying the photo-cleavable moiety.

Reaction with lipid **8** and **9** gave the lipid amidites **13** and **14**, respectively. In addition, similar lipid amidites (**15** and **16**, respectively) featuring a fluorenylmethyl (Fm) protecting or an acetoxybenzyl group on the phosphoramidite were prepared (Scheme 2). Coupling to the inositol headgroup delivered the four fully protected lipid derivatives **17a**–**d** as mixtures of diastereomers. Deprotection of the Fmoc and Fm groups in one step gave the desired caged lipids **1a**, **b**, and **d**, as well as the charged PI derivative **18**. The latter was alkylated with acetoxymethyl bromide to give the bioactivatable lipid derivative **1c**.

The caged PI derivatives were tested for cell entry and removal of the photo-activated protecting group ("uncaging"). The latter was achieved by illuminating a 10 mM sample (1 nmol in total) of **1a** (Figures 2A and Figure S2 in the Supporting Information) or **1b** (Figure S2), respectively, for 2 min in a test tube by a 1000 W lamp (Newport) equipped with a 400 nm longpass filter.

Cell entry and fluorescence levels of compounds with and without diazirine/alkyne (**1a** and **b**, respectively) were almost

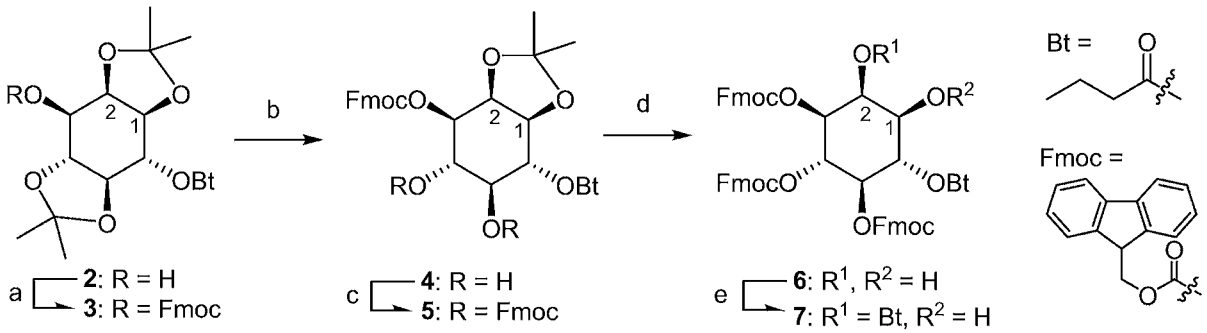


**Scheme 1.** Reagents and conditions: a) Fmoc-Cl, pyridine, $CH_2Cl_2$, 0–24 °C, 2 h, 97%; b) HCOOH/$CH_2Cl_2$ 10:34, 24 °C, 3 h, 38%; c) Fmoc-Cl, pyridine, $CH_2Cl_2$, 0–24 °C, 2 h, 98%; d) $CF_3COOH/CHCl_3$ 1:5, 24 °C, 1 h, 94%; e) 1) *n*PrC(OMe)$_3$, poly(4-vinylpyridine) $CF_3COOH$ salt, 23 °C, 20 h; 2) HCl, MeCN, THF, $H_2O$, 23 °C, 4 h, 93% yield over two steps.

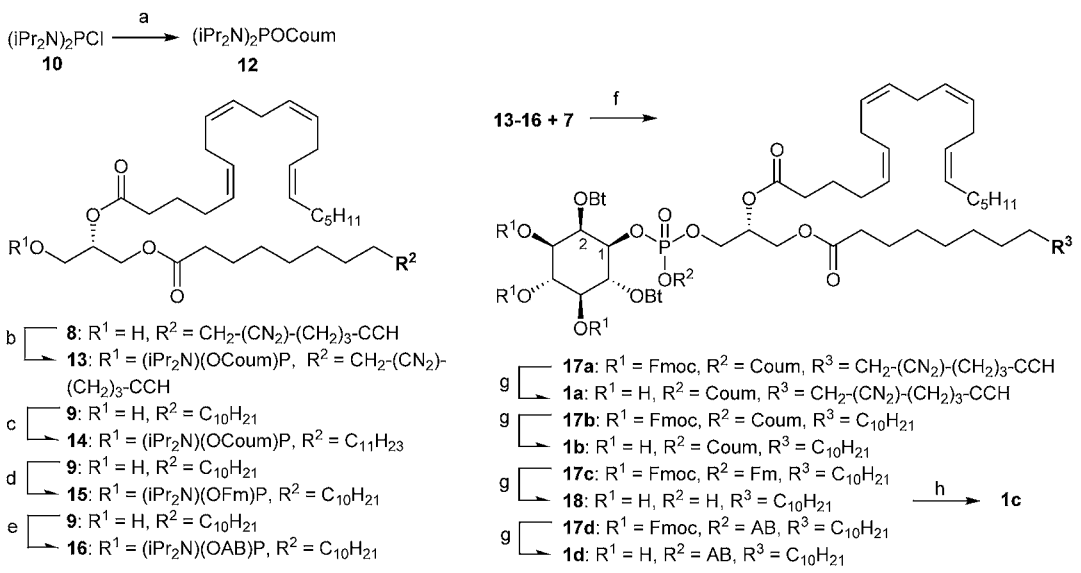


**Scheme 2.** Reagents and conditions: a) **11**, $NEt_3$, THF, 0–23 °C, 67%; b) **12**, 1*H*-tetrazole, dichloromethane (DCM), 0–23 °C, 1.5 h, 66%; c) **12**, 1*H*-tetrazole, DCM, 0–23 °C, 1.5 h, 92%; d) $(iPr_2N)_2POFm$,[14,20] 1*H*-tetrazole, $NEt_3$, DCM, 21 °C, 2 h, 94%; e) $(iPr_2N)_2POAB$,[21] 1*H*-tetrazole, DCM, 23 °C, 2 h, 88%; f) **17a–d**: 1) **13–16**, respectively, 1*H*-tetrazole, DCM, 23 °C, 2 h, 2) $AcO_2H$/AcOH, DCM, −78–23 °C, 1 h, 82–99% (two steps); g) **1a**: $Me_2NEt$, MeCN, 2 h, 65%; **1b**: $Me_2NEt$, MeCN, 2 h, 99%; **18**: $Me_2NEt$, MeCN, DCM, 1 h, not isolated,, **1c**: $Me_2NEt$, MeCN, DCM, 1 h, 84%; h) $AcOCH_2Br$, $iPr_2NEt$, MeCN, 24 °C, 16 h, 67% (two steps); **1d**: $Me_2NEt$, MeCN, 2 h, 99%. ($CN_2$) = diazirine group, AB = acetoxybenzyl.

identical, indicating that the diazirine and alkyne groups did not alter lipid properties in this respect. TLC analysis before and after showed almost complete removal of the coumarin group of **1a** (Figure 2A). Caged lipid **1a** and its uncaged version were detected after tagging with fluorogenic 3-azido-7-hydroxy-coumarin (**19**). Similarly, we performed pulse chase experiments of **1a** after incubating HeLa cells for up to two hours. In the absence of irradiation >400 nm, very little decrease in lipid levels were detected by TLC (Figure 2B and C). After uncaging, there was a significant decrease in the PI spot, potentially due to metabolism to higher phosphorylated phosphoinositides (Figure 2B and C ). This result demonstrates that the cage successfully prevents metabolism. Because the caged lipid derivatives are fluorescent, we observed cell entry into HeLa cells by confocal fluorescence microscopy on an Olympus FV1200 confocal microscope (Figure 3).

Cells were incubated with 10 μM **1a** (or **1b**, respectively, Figure S1 in the Supporting Information) in the presence of the non-ionic detergent pluronic F-127 for 30 seconds, 5.5, and 30.5 minutes. As was expected, loading of cells with **1a** was rapid. A maximum amount of lipid was detected after 5 minutes. The fluorescence of the caged lipid was visible in all endomembranes (Figure 3A). This is a typical phenomenon that seems to stem from the cage itself and has been observed for other fluorescently tagged lipid derivatives.[18,22] Subsequent illumination with 405 nm to remove the cage led to a strong increase of fluorescence. This effect is known for other coumarin-caged molecules,[23] because the released hydroxymethyl coumarin **11** has a significantly higher quantum yield than the caged molecule (Figure 3B). Subsequently, the released coumarin likely leaves the cells leading to a decrease in cell fluorescence.

To provide proof-of-concept that photo-cross-linking in intact HeLa cells will reveal the location of the cross-linked lipid–protein complexes at the moment of illumination, we incubated cells with 10 μM of **1a** for 5 minutes. After uncaging with or without subsequent photo-cross-linking, cells were fixed and the covalent lipid–protein conjugates were fluorescently tagged with Alexa 488—picolyl azide. We performed the uncaging reaction with >400 nm light for 2 minutes via a 1000 W Xenon lamp (Newport). Subsequently, we illuminated cells with >345 nm light for 2 min with the same lamp (Figure 4B). Control cells were only uncaged at >400 nm for 4 minutes (Figure 4A). Cells were fixed in methanol and subsequently washed with methanol/chloroform/acetic acid (55:10:0.75), which removed most of the non-cross-linked lipids, as well as the released coumarin. As depicted in Figure 4B, cells illuminated with >345 nm light showed significant fluorescence indicating that photo-cross-linking to proteins was successful.

Interestingly, with increased uncaging times, cells were successively more stained at the plasma membrane, a location significantly different from the location of the intact caged lipid (Figure 4B). This indicates that between uncaging and photo-cross-linking, the lipid was transferred to the plasma membrane as was described for endogenous PI.[4] It seems that the uncaged lipid is accepted by the major PI transfer proteins PITPα and PITPβ (see below).

To confirm lipid specificity, we co-incubated cells with a low amount (5 μM) of the photo-cross-linkable PI derivative **1a**, as well as with a higher amount (25 μM) of the non-caged AM ester **1c**, a derivative with a natural fatty acid composition, or the respective caged derivative **1b**. As shown in Figure 5, PI delivered by the AM ester **1c** fully and **1b** partially outcompet-

 

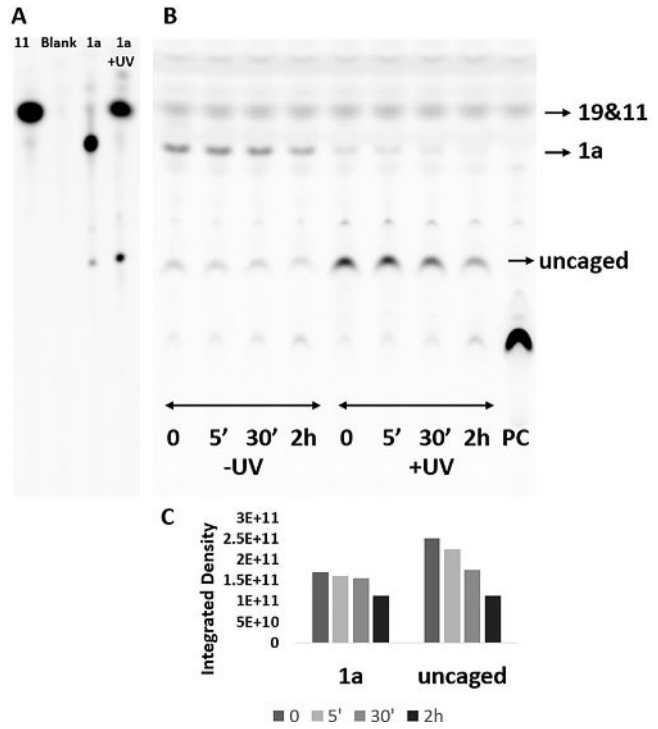


**Figure 2.** TLC of caged and uncaged PI derivatives on HPTLC silica 60. Extracted lipids were labeled with 3-azido-7-hydroxy-coumarin (**19**) via copper-catalyzed click chemistry. A) 10 mM stock of coumarin **11**, the molecule released after uncaging **1 a** (left lane); 10 mM stock solution of **1 a** in MeOH (third lane) and the same after illumination with >400 nm (fourth lane). The small spot in lane 3 at the level of compound **11** might occur due to a marginal instability of the phosphate triester in **1 a**. B) Extracts from HeLa cells initially treated with 10 μM **1 a** for 5 min, with and without subsequent UV illumination ($t=0$) followed by incubation in fresh buffer for the times indicated. Without uncaging (−UV), little change was observed, whereas after uncaging (+UV), a significant decrease in PI was detected over time. C) Lipid spots corresponding to compound 1 in −UV condition (**1**) and the lipid spots corresponding to the uncaged derivative in +UV condition (uncaged) in B were quantified for $t=0$, 5′, 30′, 2 h. Integrated densities were plotted following background subtraction.

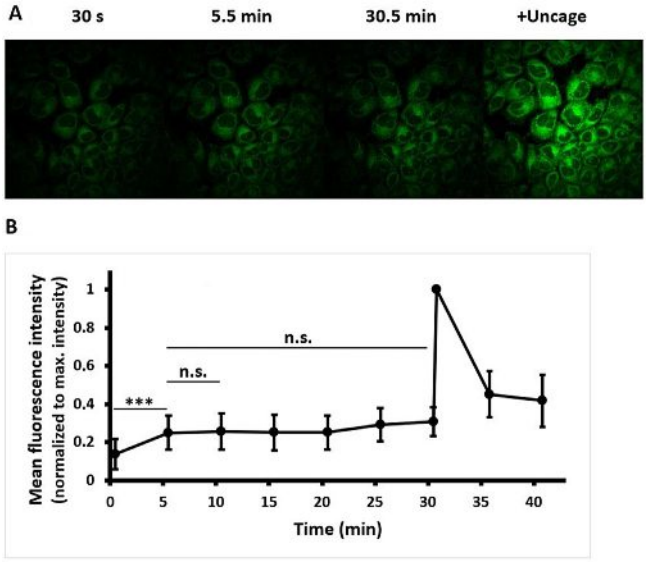


**Figure 3.** Cell entry. A) Images of HeLa cells incubated with **1 a** for 30 s, 5.5 and 30.5 min, as well as after uncaging with 405 nm light for 20 s (30.8 min). B) Mean fluorescence intensities from whole surface area of single cells were measured following background subtraction from images of HeLa cells incubated with **1 a** at various time points and after uncaging at 30.8 min. Note the decrease in fluorescence after the initial spike due to diffusion of the released coumarin. The fluorescence intensities at each time point were normalized to the maximum fluorescence intensity measured right after uncaging at 30.8 min. Error bars represent standard deviation. Statistical significance was evaluated using unpaired, two-tailed Student's t-test ($n=16$ cells from four independent dishes, ***: $p<0.001$, n.s. = not significant).

ed the PI binding sites resulting in marginal membrane staining after photo-cross-linking. This result suggested that the AM ester **1 c** was successfully entering cells and after AM ester cleavage outcompeted the multifunctional PI derivative. It should be mentioned that the AM ester seems to reach higher concentrations due to the negative charge on the phosphate after hydrolysis while the uncharged caged molecules enter

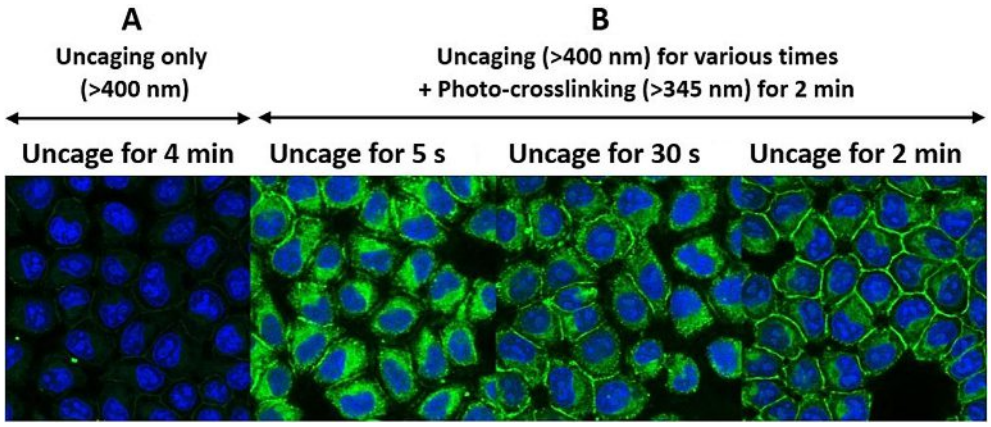


**Figure 4.** Photo-cross-linked PI location. A) HeLa cells were incubated with 10 μM **1 a** for 5 min and uncaged with >400 nm light for 4 min without photo-cross-linking. Subsequently, cells were fixed in 100% cold methanol. Non-cross-linked lipids and cleaved coumarin were extracted with methanol/chloroform/acetic acid (55:10:0.75). Lipid location was determined via click chemistry of Alexa 488—picolyl azide (green). Cells were counterstained with DAPI (blue). B) HeLa cells were incubated with 10 μM **1 a** for 5 min and uncaged for 5 s, 30 s, or 2 min with >400 nm light prior to illumination with >345 nm light for 2 min to induce photo-cross-linking. Samples were processed as in A. Note the increase in ratio of plasma membrane staining to internal membrane staining due to longer uncaging times before cross-linking.

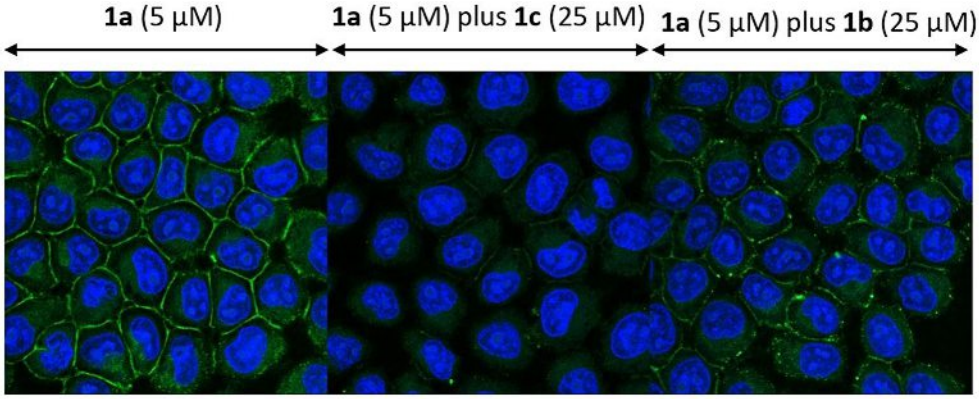


**Figure 5.** Incubation of the photo-cross-linkable derivative **1 a** in the presence of a higher amount of membrane-permeant non-caged and non-cross-linkable PI **1 c** (middle) or the caged, non-cross-linkable derivative **1 b** resulted in much reduced staining of membranes after successive applications of uncaging with >400 nm light for 2 min and photo-cross-linking with >345 nm light for 2 min, fixation, extraction, and subsequent staining with Alexa 488—picolyl azide (green) and DAPI (blue). The images are representative of three independent experiments.

and leave cell membranes thereby producing a steady state within about 5 minutes (Figure 3).

To demonstrate that transport of PI was responsible for the location change within minutes after uncaging, we pulled down the photo-cross-linked PI-protein conjugates from HeLa cell lysates with picolyl azide-coated beads by click chemistry. Preliminary proteomic analysis showed that both PITP isoforms were significantly enriched (Table 1). This result supports our hypothesis that the PI derivatives we deliver to cells are transported from endomembranes to the plasma membrane through the endogenous transport proteins.

**Table 1.** Quantitative values for spectral counts from normalized total spectra (minimum value was set to 1 in case spectra were absent) in + UV (>400 nm for 2 min and >345 nm for 2 min) and −UV (only >400 nm for 4 min) conditions, and fold increase of PI transport proteins after photo-cross-linking.

| | Spectral counts in −UV | Spectral counts in +UV | Fold increase |
|---|---|---|---|
| PITPβ | 3.08 | 77.7 | 25.2 |
| PITPα | 1.00 | 6.58 | 6.58 |

In conclusion, we synthesized the first membrane-permeant and caged derivatives of PI. The 7-diethylaminocoumarin-based caging group is well established.[11,22,23] It can be very rapidly removed from phosphates with blue light.[22] In fact, one of the advantages of this type of cage over nitrobenzyl-based caging groups is the light-induced radical mechanism that leads to very fast release kinetics. In addition to the caging group, we equipped the PI derivative with a photo-cross-linkable diazirine not sensitive to the uncaging light and an alkyne group for click chemistry. Although the caging group is intended to prevent premature metabolism, the diazirine group permits specific fixation of the lipid derivative to its binding proteins. This is particularly important when cells are fixed for subsequent inspection under the microscope because many fixation conditions fully or partially remove small molecules including lipids. Click chemistry then permits tagging with fluorophores or attachment to azide-bearing beads for the isolation of lipid–protein conjugates. In this work, we demonstrated that all introduced functionalities performed well. We confirmed that caged PI was intrinsically targeted to endomembranes, likely due to the aromatic nature of the coumarin group, but that the removal of the caging group permitted a rapid transport to the plasma membrane as was described for endogenous PI. In fact, the release of PI at endomembranes allowed us to monitor PI transport in intact cells. Future work might provide a quantitative evaluation of this PI transport via transport proteins. It should be noted that uncaging of **1 a** is likely generating not only the modified PI but also its mono- and/or dibutyrate. To date, it is unclear if these esters will also be transported. Future mass spectrometry analysis will help to answer this question.

Multifunctional derivatives of drug molecules equipped with photo-cross-linkable and alkyne groups are frequently used in the pharmaceutical industry to identify drug candidate targets in living cells.[24–26] Similarly, the first datasets describing lipid–protein interactomes for lipids, such as diacylglycerol and sphingosine, have been presented before.[5,6,17] This work, for the first time, applies the technique successfully to a phosphoinositide. A more global future proteomic analysis of PI-binding proteins might reveal new targets that will help to elucidate cellular functions of PI beyond serving as a biosynthetic precursor for the higher phosphorylated phosphoinositides.

## Acknowledgements

We are grateful for financial support by the Deutsche Forschungsgemeinschaft (Transregio 83 and 186). CS is partially funded by the NIH R01GM127631. The authors thank for excellent support by EMBL's Advanced Light Microscopy and Proteomic Core Facilities.

 

## Conflict of interest

The authors declare no conflict of interest.

**Keywords:** crosslinking · cellular labelling · phosphates · photochemistry

[1] V. Laketa, S. Zarbakhsh, A. Traynor-Kaplan, A. Macnamara, D. Subramanian, M. Putyrski, R. Müller, A. Nadler, M. Mentel, J. Saez-Rodriguez, R. Pepperkok, C. Schultz, *Sci. Signaling* **2014**, *7*, ra5.

[2] A. Nadler, G. Reither, S. Feng, F. Stein, S. Reither, R. Müller, C. Schultz, *Angew. Chem. Int. Ed.* **2013**, *52*, 6330 – 6334; *Angew. Chem.* **2013**, *125*, 6455 – 6459.

[3] A. H. Lystad, A. Simonsen, *FEBS Lett.* **2016**, *590*, 2454 – 2468.

[4] A. Grabon, V. A. Bankaitis, M. I. McDermott, *J. Lipid Res.* **2019**, *60*, 242 – 268.

[5] P. Haberkant, R. Raijmakers, M. Wildwater, T. Sachsenheimer, B. Brugger, K. Maeda, M. Houweling, A. C. Gavin, C. Schultz, G. van Meer, A. J. Heck, J. C. Holthuis, *Angew. Chem. Int. Ed.* **2013**, *52*, 4033 – 4038; *Angew. Chem.* **2013**, *125*, 4125 – 4130.

[6] P. Haberkant, F. Stein, D. Höglinger, M. J. Gerl, B. Brugger, P. P. Van Veldhoven, J. Krijgsveld, A. C. Gavin, C. Schultz, *ACS Chem. Biol.* **2016**, *11*, 222 – 230.

[7] D. Höglinger, P. Haberkant, A. Aguilera-Romero, H. Riezman, F. D. Porter, F. M. Platt, A. Galione, C. Schultz, *eLife* **2015**, *4*, e10616.

[8] C. Schultz, *Bioorg. Med. Chem.* **2003**, *11*, 885 – 898.

[9] C. Schultz, M. Vajanaphanich, A. T. Harootunian, P. J. Sammak, K. E. Barrett, R. Y. Tsien, *J. Biol. Chem.* **1993**, *268*, 6316 – 6322.

[10] S. Hauke, A. K. Dutta, V. B. Eisenbeis, D. Bezold, T. Bittner, C. Wittwer, D. Thakor, I. Pavlovic, C. Schultz, H. J. Jessen, *Chem. Sci.* **2019**, *10*, 2687 – 2692.

[11] D. Höglinger, A. Nadler, C. Schultz, *Biochim. Biophys. Acta Mol. Cell Biol. Lipids* **2014**, *1841*, 1085 – 1096.

[12] C. Dinkel, M. Moody, A. Traynor-Kaplan, C. Schultz, *Angew. Chem. Int. Ed.* **2001**, *40*, 3004 – 3008; *Angew. Chem.* **2001**, *113*, 3093 – 3096.

[13] M. Mentel, V. Laketa, D. Subramanian, H. Gillandt, C. Schultz, *Angew. Chem. Int. Ed.* **2011**, *50*, 3811 – 3814; *Angew. Chem.* **2011**, *123*, 3895 – 3898.

[14] D. Subramanian, V. Laketa, R. Müller, C. Tischer, S. Zarbakhsh, R. Pepperkok, C. Schultz, *Nat. Chem. Biol.* **2010**, *6*, 324 – 326.

[15] M. Bartsch, M. Zorn-Kruppa, N. Kuhl, H. G. Genieser, F. Schwede, B. Jastorff, *Biol. Chem.* **2003**, *384*, 1321 – 1326.

[16] W. H. Li, C. Schultz, J. Llopis, R. Y. Tsien, *Tetrahedron* **1997**, *53*, 12017 – 12040.

[17] D. Höglinger, A. Nadler, P. Haberkant, J. Kirkpatrick, M. Schifferer, F. Stein, S. Hauke, F. D. Porter, C. Schultz, *Proc. Natl. Acad. Sci. USA* **2017**, *114*, 1566 – 1571.

[18] A. Laguerre, C. Schultz, *Curr. Opin. Cell Biol.* **2018**, *53*, 97 – 104.

[19] M. Leutert, D. M. L. Pedrioli, M. O. Hottiger, *Mol. Cell* **2016**, *63*, 181 – 183.

[20] C. Dinkel, O. Wichmann, C. Schultz, *Tetrahedron Lett.* **2003**, *44*, 1153 – 1155.

[21] A. Routledge, I. Walker, S. Freeman, A. Hay, N. Mahmood, *Nucleosides Nucleotides* **1995**, *14*, 1545 – 1558.

[22] V. Hagen, J. Bendig, S. Frings, T. Eckardt, S. Helm, D. Reuter, U. B. Kaupp, *Angew. Chem. Int. Ed.* **2001**, *40*, 1045 – 1048; *Angew. Chem.* **2001**, *113*, 1077 – 1080.

[23] G. Mayer, A. Heckel, *Angew. Chem. Int. Ed.* **2006**, *45*, 4900 – 4921; *Angew. Chem.* **2006**, *118*, 5020 – 5042.

[24] P. L. D'Alessandro, N. Buschmann, M. Kaufmann, P. Furet, F. Baysang, R. Brunner, A. Marzinzik, T. Vorherr, T. M. Stachyra, J. Ottl, D. E. Lizos, A. Cobos-Correa, *Angew. Chem. Int. Ed.* **2016**, *55*, 16026 – 16030; *Angew. Chem.* **2016**, *128*, 16260 – 16264.

[25] D. S. Tyler, J. Vappiani, T. Caneque, E. Y. N. Lam, A. Ward, O. Gilan, Y. C. Chan, A. Hienzsch, A. Rutkowska, T. Werner, A. J. Wagner, D. Lugo, R. Gregory, C. Ramirez Molina, N. Garton, C. R. Wellaway, S. Jackson, L. MacPherson, M. Figueiredo, S. Stolzenburg, C. C. Bell, C. House, S. J. Dawson, E. D. Hawkins, G. Drewes, R. K. Prinjha, R. Rodriguez, P. Grandi, M. A. Dawson, *Science* **2017**, *356*, 1397 – 1401.

[26] A. Rutkowska, D. W. Thomson, J. Vappiani, T. Werner, K. M. Mueller, L. Dittus, J. Krause, M. Muelbaier, G. Bergamini, M. Bantscheff, *ACS Chem. Biol.* **2016**, *11*, 2541 – 2550.

Manuscript received: August 13, 2019
Revised manuscript received: September 22, 2019
Accepted manuscript online: September 24, 2019
Version of record online: December 6, 2019

 